INVESTIGATION OF DENSITY LIMIT PROCESSES IN DIII–D[*]

R. MAINGI,[†] M.A. MAHDAVI, T.W. PETRIE, L.R. BAYLOR,[†] J.W. CUTHBERTSON,[‡]
D.N. HILL,[Δ] A.W. HYATT, T.C. JERNIGAN,[†] R.J. LA HAYE, C.J. LASNIER,[Δ]
A.W. LEONARD, M. MURAKAMI,[†] R.T. SNIDER, R.D. STAMBAUGH, D.M. THOMAS,
M.R. WADE,[†] J.G. WATKINS,[◊] W.P. WEST,and D.G. WHYTE[‡]
DIII–D National Fusion Facility, General Atomics, San Diego, California, U.S.A.

Abstract

A series of experiments has been conducted in DIII–D to investigate density-limiting processes. We have studied divertor detachment and MARFEs on closed field lines and find semi-quantitative agreement with theoretical calculations of onset conditions. We have shown that the critical density for MARFE onset at low edge temperature scales as I_p/a^2, i.e. similar to Greenwald scaling. We have also shown that the scaling of the critical separatrix density with heating power at partial detachment onset agrees with Borass' model. Both of these processes yield high edge density limits for reactors such as ITER. By using divertor pumping and pellet fueling we have avoided these and other processes and accessed densities $> 1.5\times$ Greenwald limit scaling with H–mode confinement, demonstrating that the Greenwald limit is not a fundamental limit on the core density.

Density limit studies and projections are crucial in the design of a fusion reactor's basic operational regime. The operating plasma temperature is set by reactivity considerations. Thus the plasma density, in particular the density in the high reactivity region, determines the fusion power production for an optimized plasma temperature. In present day tokamaks in the high confinement mode (H–mode), the density profiles are relatively flat and it is difficult to create a peaked density profile with H–mode level energy confinement. This flatness of the profile has an undesirable consequence: achievement of a high density core requires a high density edge plasma. However, it is precisely the edge region which can impose the lowest absolute density limit. Thus achievement of a high central density can be restricted by edge density limits.

Historically density limits have been measured and cited as limits on the line-average density ($\bar{n}_e$) measured with an interferometer chord, preventing conclusive identification of the underlying mechanisms. Studies [1,2] of multi-machine databases have identified a commonly observed density limit scaling: $\bar{n}_e \propto I_p/a^2$, where I_p is the plasma current and a is the minor radius. However extrapolation of this scaling to reactors can be misleading because the underlying processes have not been definitively determined. The scaling has consequences for fusion reactors: many D-T reactor designs must operate above this limit for economic competitiveness. Theories indicate that several distinct processes exist which can limit density in either the core, edge, or divertor plasma. Motivated by the International Thermonuclear Experimental Reactor's (ITER) need [3] to operate with density above the Greenwald limit (n_{GW}) [2] with H–mode energy confinement, a multi-year experimental campaign has been carried out in DIII–D to identify density-limiting processes and determine techniques to avoid them [4]. Here density "limit" is used loosely since we include processes which prevent attainment of high density operation *with* high energy confinement, as opposed to exclusively disruptive processes. One of our primary goals was to separate edge and core density limit mechanisms.

A density limit in H–mode discharges is most easily observed in a density ramp with external gas fueling. In DIII–D, the following time sequence is usually observed as $\bar{n}_e$ is increased:

[†]Oak Ridge National Laboratory.
[‡]University of California, San Diego.
[Δ]Lawrence Livermore National laboratory.
[◊]Sandia National Laboratories, Albuquerque.

1. The divertor plasma partially detaches [5] from the outer target plate upon crossing a private flux region neutral pressure limit [6] and a divertor "MARFE" forms on the low-field side of the X–point region
2. The divertor plasma completely detaches, i.e. the divertor D_α and target particle flux are reduced to ~ 0
3. The divertor "MARFE" begins to migrate to closed field lines
4. An H–mode-to-L–mode confinement transition is observed ELM activity ceases, and the MARFE encroaches onto closed field lines in the X–point area

This entire sequence was eliminated [4] by active pumping of the divertor with the in-vessel cryopump. Pumping maintained the private region neutral pressure below the critical value [6] for partial detachment onset. Pellet fueling replaced gas fueling to raise the plasma density while maintaining low divertor neutral pressure.

Partial detachment [5] is in fact an attractive reactor operating scenario because of reduced heat flux without deleterious confinement effects. Borass' 2-point SOL and divertor plasma model has been benchmarked [7] with experimental data from existing tokamaks and used to predict conditions required for detachment onset for ITER. This model was applied [8] to DIII–D conditions and predicted a power scaling of the critical usptream separatrix density and temperature (n_{upst}^{crit} and T_{upst}^{crit}) for partial detachment onset: $n_{upst}^{crit} \propto P_{div,outer}^{0.7}, T_{upst}^{crit} \propto P_{div,outer}^{0.3}$, where $P_{div,outer}$ is the power flow into the outer divertor. The upstream parameters when the divertor temperature, T_{div}, falls below 5 eV were taken as the partial detachment onset point in the modeling. Figure 1 shows that experimentally $n_{upst}^{crit} \propto P_{div,outer}^{0.76}, T_{upst}^{crit} \propto P_{div,outer}^{0.57}$, from Thomson Scattering measurements of electron parameters just above the outer midplane at partial detachment onset. Thus the predicted density scaling appears to fit our data but the temperature dependence is stronger than predicted by the model. Also, the absolute upstream separatrix density predicted by the model is about 2× higher than our measured values — more work is required to understand this particular discrepancy. This study demonstrates the importance of local parameter analysis for these processes: we have previously reported [9] that the critical $\bar{n}_e$ for detachment onset is almost insensitive to the global heating power, i.e. $\bar{n}_e^{crit} \propto P_{heat}^{0.15}$. In fact that same dependence is present in these data but the global analysis masks the important dependencies. The reason is quite simple: gas puffing preferentially raises the SOL density relative to $\bar{n}_e$. Thus while the changes in the $\bar{n}_e$ are small during these scans, the SOL density increases much more rapidly.
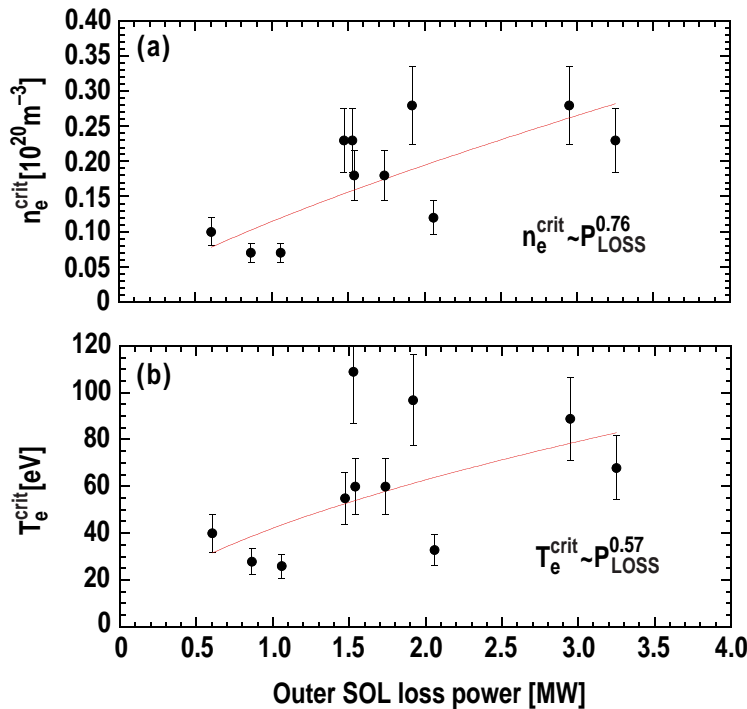

FIG. 1. Scaling of (a) critical separatrix density and (b) temperature at detachment onset as a function of the loss power to the outer divertor.

The high density H–L back transition is often accompanied [4,10,11] by MARFEs on closed field lines just inside of the X–point region. In DIII–D this transition is usually observed at between 0.7–1.0*Greenwald scaling. We have formulated the MARFE onset criterion for DIII–D discharge parameters and shown [12] that a discharge with a MARFE was predicted to be unstable to MARFE formation, whereas a discharge without a MARFE was predicted to be stable. In the low edge temperature region near the separatrix for T_e<75 eV, the MARFE onset critical density increases as the edge T_e^4, primarily because of the $T_e^{7/2}$ dependence of the parallel heat flux which can stabilize the radiative cooling mechanism responsible for the MARFE. When combined with the ITER-89P scaling law for L–mode energy confinement, it can be shown[1] [12] that the MARFE onset critical upstream electron density (n_e^{crit}) has the following scaling:

$$n_e^{crit} \propto \frac{I_p^{0.96}}{a^{1.9}} \xi^{-0.11} P_{heat}^{0.43} R_m^{0.17} B_t^{0.04} (\kappa^2 (1 + \kappa^2))^{-0.22} \qquad (1)$$

where ξ is impurity concentration, P_{heat} is the heating power, R_m is the major radius, B_t is the toroidal field, and κ is the elongation. This scaling is remarkably similar to Greenwald, both in the strong I_p and a dependencies but also in the weak dependencies on other quantities (except P_{heat}). Thus the scaling is clearly applicable to L–mode plasmas which usually have T_e<100 eV at the edge. H–mode confinement scaling laws have similar dependencies on engineering parameters, leading to a similar scaling for high density ELMY H–mode plasmas in DIII–D. Note that the scaling above predicts a stronger dependence on P_{heat} than observed on present day machines — we speculate that this discrepancy is related to global parameter analysis presented in most density limit studies and global confinement scaling used to arrive at Eq. (1). This scaling yields an edge plasma density limit which should be of no concern for reactors such as ITER which are expected to operate at edge temperatures well above 100 eV.

After eliminating the detachment and MARFE sequence with divertor pumping, pellet injection was used to fuel the core. However, pellet fueling characteristics lead to other restrictions [4] in the high-density operational window. We observed a stronger than linear plasma current dependence of the density decay time following pellet injection, which suggested operation at high I_p was favorable for increasing density. In contrast to Greenwald's original analysis [2], we found no correlation between the density decay time and $\bar{n}_e/n_{GW}$. In addition, pellet fueling efficiency was found to decrease with heating power, suggesting low heating power was favorable. At B_t =2.15 T the heating power was $\leq 2 \times$ L-H confinement transition power threshold. In this regime pellets produced H-L transitions which rapidly ejected the pellet density in <10 ms. Access to high density was achieved by operating at low B_t, giving more margin over the L-H threshold. We found that MHD modes could be de-stabilized at densities as low as $\bar{n}_e/n_{GW} \sim 0.8$ during pellet fueling. The n=2 modes resulted in tolerable particle and energy confinement degradation (10%–15%), but the n=1 modes were catastrophic. The cause for the onset of these MHD modes is unclear, but the n=1 modes were avoided by operating at P_{heat}< 3 MW ($\beta_N \leq 1.7$).

By studying each of the aforementioned physical processes and selecting conditions to avoid them, we have achieved discharges (e.g. Fig. 2) for the first time at $\bar{n}_e/n_{GW} \geq 1.5$ for up to 600 ms, with a peak energy confinement time of ~1.2*ITER93H scaling. Due to the operating conditions required [4], these discharges were ELM-free and suffered from core impurity accumulation and a central power balance limit. Our effectiveness in heating the center was limited by the neutral beam technique; the heating deposition became peaked well off-axis during the high density phase, leading to a central radiative loss rate 4–5 times larger than the neutral beam heating rate. The central power balance density limit has been shown to be very high for reactors in which the heating profile will always be peaked on-axis.

In summary, the various edge density limits we have studied all extrapolate favorably for ITER. By avoiding the pellet fueling, confinement, and MHD limits, we were able to successfully achieve the central core radiative collapse density limit. This limit has been shown to be very high for ITER. The focus of present studies is on understanding the various pellet-fueling related limits. In addition,

---

[1]Note that this paper erroneously reported $n_e^{crit} \propto P_{heat}^{0.17}$; the correct relation is $n_e^{crit} \propto P_{heat}^{0.43}$.
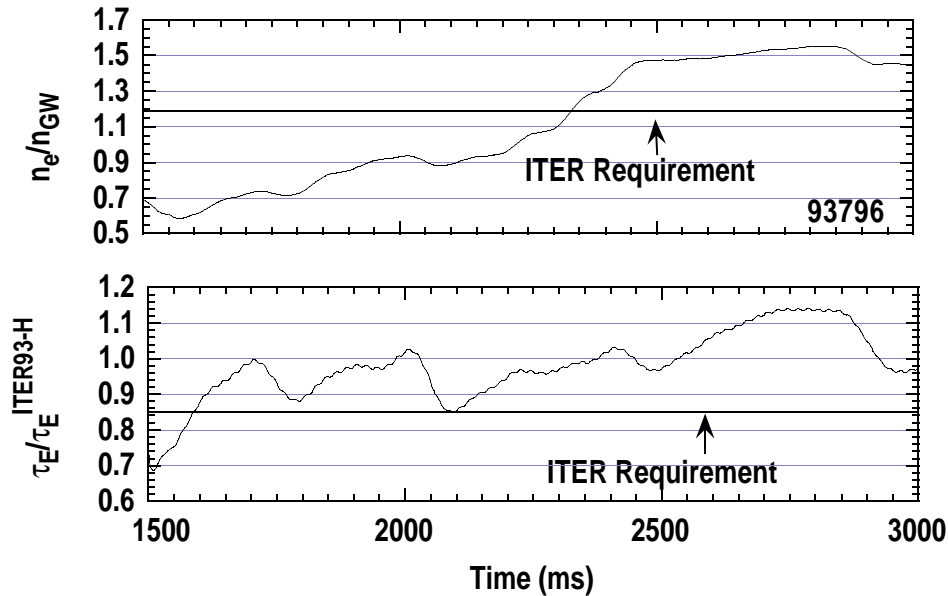
FIG. 2. Demonstration discharge with density ≥ 1.5× Greenwald scaling and H–mode confinement.

injection from the high-field side has been shown [13] to increase fueling efficiency at high heating power which should allow us to raise the maximum $\beta_N > 2$, ITER's high value. This capability has been installed into DIII–D and will be used in upcoming experiments.

REFERENCES

[1]   HUGHILL, J., *et. al*., in Heating in Toroidal Plasmas (Proc. 2nd Joint Varenna-Grenoble Int. Symp., Como, 1980), Vol. 2, CEC, Brussels (1980) 775.
[2]   GREENWALD, M., *et. a*l., Nucl. Fusion **2**, 2199 (1988).
[3]   PERKINS, F.W., *et. al.*, Proc. 16th International Fusion Energy Conference, October 7–11, 1996, Montreal, Canada, paper F1-CN-64/FP-24.
[4]   MAINGI, R., *et al.,* Phys. Plasmas **4** (1997) 1752.
[5]   PETRIE, T.W., *et. al.*, Nucl. Fusion **37** (1997) 321.
[6]   GRENDRIH, P., *et. al.*, J. Nucl. Mater. **220-222** (1995) 305.
[7]   BORASS, K., Nucl. Fusion **31** (1991) 1035.
[8]   MAINGI, R., *et al.,* Proc. of 13th International Conf. on Plasma Surface Interactions, San Diego, CA, May 18-23, 1998, *J. Nucl. Mater.* in press.
[9]   PETRIE, T.W., *et. al.*, Nucl. Fusion **33** (1993) 929.
[10]   PETRIE, T.W., *et. al.*, J. Nucl. Mater. **241–243** (1997) 639.
[11]   MERTENS, V., *et. al.*, Proc. 16th International Fusion Energy Conference, October 7-11, 1996, Montreal, Canada, paper F1-CN-64/A4-4.
[12]   MAHDAVI, M.A., *et al.*, presented at 24th Euro. Conf. on Contr. Fusion and Plasma Phys. June 9-14, 1997, Berchtesgaden, Germany.
[13]   LANG, P.T., et al., Phys. Rev. Lett **79** 1487 (1997).